ACTA ABP BIOCHIMICA POLONICA

Vol. 68, No 1/2021
115–118
https://doi.org/10.18388/abp.2020_5465

Regular paper

Abundance, fatty acid composition and saturation index of neutral lipids in colorectal cancer cell lines

Rimsha Munir[1,2], Jan Lisec[3], Carsten Jaeger[3] and Nousheen Zaidi[1,2]✉

[1]Cancer Biology Lab, Institute of Microbiology and Molecular Genetics, University of the Punjab, Lahore, Pakistan; [2]Cancer Research Centre (CRC), University of the Punjab, Lahore, Pakistan; [3]Bundesanstalt für Materialforschung und -prüfung (BAM), Berlin, Germany

Lipid droplets, the dynamic organelles that store triglycerides (TG) and cholesterol esters (CE), are highly accumulated in colon cancer cells. This work studies the TG and CE subspecies profile in colon carcinoma cell lines, SW480 derived from primary tumor, and SW620 derived from a metastasis of the same tumor. It was previously reported that the total TG and CE content is dramatically higher in SW620 cells; however, TG and CE subspecies profile has not been investigated in detail. The work presented here confirms that the total TG and CE content is significantly higher in the SW620 cells. Moreover, the fatty acid (FA) composition of TG is significantly altered in the SW620 cells, with significant decrease in the abundance of saturated triglycerides. This resulted in a significantly decreased TG saturation index in the SW620 cells. The saturation index of CE was also significantly decreased in the SW620 cells.

Keywords: Cancer metabolism, colon cancer, fatty acid saturation, lipid droplets, lipidomics, triglycerides.

Received: 26 August, 2020; revised: 21 October, 2020; accepted: 30 October, 2020; available on-line: 17 February, 2021

✉e-mail: nosheen.mmg@pu.edu.pk
Acknowledgements of Financial Support: This work was supported by the Alexander von Humboldt Foundation.
Abbreviations: CE, cholesterol ester; CRC, colorectal cancer; LDs, lipid droplets; TG, total triglyceride; PUFAs, polyunsaturated fatty acids

INTRODUCTION

Lipidomic landscape of colorectal cancer (CRC) cells is significantly modified in comparison to that of their non-malignant counterparts (Pakiet *et al.*, 2019). Primary and metastatic colon cancer cells also display a difference in their lipidomic profiles (Fhaner *et al.*, 2012). Previous works have taken advantage of the SW480/SW620 cell line pair, which represents an accepted model to study metastatic progression (Hewitt *et al.*, 2000). SW480 is derived from a primary tumor, and SW620 is derived from a metastasis of the same tumor (Leibovitz *et al.*, 1976). Multiple differences in the lipidomic profiles of these two cell lines have been noted (Fhaner *et al.*, 2012). It has been shown that the SW620 cells display a dramatic increase in the total triglyceride (TG) and cholesterol ester (CE) levels (Fhaner *et al.*, 2012). However, the TG and CE subspecies profiles have not been explored in detail. Studying the TG and CE profile of CRC cells is particularly important because these neutral lipids form hydrophobic core of lipid droplets (LDs) that are highly accumulated in the CRC cells (Tirinato *et al.*, 2015). Previous works have shown that exposure to excessive polyunsaturated fatty acids (PUFAs) induces LD formation in both, the SW480 and SW620 cells (Schonberg *et al.*, 2006). Interestingly, the SW620 cells accumulate PUFA-enriched CE, while the SW480 cells accumulate PUFA-enriched TG (Schonberg *et al.*, 2006). Herein, we studied the differences in the TG- and CE-subspecies profiles and saturation index (SI) between the SW480 and SW620 cells. Moreover, expression of various metabolic genes that may bring about these lipidomic changes was also analyzed.

MATERIALS AND METHODS

Gene Expression Analysis

Quantitative RT-PCR was performed *via* StepOne Real-Time PCR Systems (Applied Biosystems) as described previously (Lisec *et al.*, 2019). Microarray data were obtained from publicly accessible gene expression profile database, GEO (data accessible at NCBI GEO database, accession number GSE2509).

Determination of Total Triglyceride and Cholesterol Ester Content

Total triglyceride content was determined using a commercially available kit (Analyticon Biotechnologies AG) against a calibration-curve generated using a triglyceride standard (SUPELCO). Cholesteryl esters were quantified using Cholesterol/ Cholesteryl Ester Quantitation Kit (Abcam).

Lipidomic Profiling and Data Analysis

Lipids were extracted and lipidomic profiling was performed as described previously (Lisec *et al.*, 2019). For each of 6 replicate samples per cell line we calculated the relative distribution of lipids containing none (SFA0), exactly one (SFA1) and two or more saturated fatty acids (SFA2) within each major lipid class. To this end, the measured ion intensities for the groups (SFA0, 1 and 2) were summed up and normalized to the total sum of this lipid class. Mean values and standard deviations for the SFA distribution were calculated over the 6 replicates per cell line. Saturation indices were calculated as a ratio of total saturated fatty acid content to total unsaturated fatty acid content (Ackerman *et al.*, 2018) within each major lipid class. Total content of saturated fatty acids was calculated by summing up the intensities of all lipids multiplied by the number of saturated fatty acids present within each lipid. Total content of unsaturated fatty acids in each individual lipid class was calculated by summing up the intensities of

all lipids multiplied by the number of unsaturated fatty acids present within each lipid. To compare SI over lipid classes we normalized with respect to the SI value obtained for SW480.

Statistical analysis

The differences between groups were analyzed by ANOVA or t-test (paired or unpaired), where applicable. *P*-values<0.05 were considered statistically significant and are indicated when different.

RESULTS AND DISCUSSION

First, we assessed the total TG and CE content and observed that the SW620 cells display 2.5-3 fold increase in the levels of these storage lipids (Supplementary Fig. 1 at https://ojs.ptbioch.edu.pl/index.php/abp/). Next, the fatty acid (FA) composition of TG and CE was compared. We observed that in the SW480 cells the triglycerides (TG) with ≥2 saturated fatty acids (SFA) were in the highest proportion (i.e. 61%). The proportion of TG containing 1 or 0 SFA was 35% and 4%, respectively. These proportions were significantly altered in the SW620 cells in which the proportion of TG with ≥2 saturated fatty acids was decreased to 40%, while the proportions of TG containing 1 or 0 SFA were increased to 53% and 7%, respectively. The saturation indices of different lipid classes are normalized to SW480. In agreement with these results, the TG saturation index (SI) was markedly higher in the SW480 cells than in the SW620 cells. On the other hand, FA-composition and SI of diglycerides, the direct precursors of TG, was only slightly altered. The FA-composition of CE also showed minor changes, with slight shift in the proportions of CE containing 0 or 1 SFA. However, the SI of CE was also significantly decreased in the SW620 cells. We also compared the FA composition of the most abundant membrane lipids, phosphatidylcholines and phosphatidylethanolamine, in the SW480 and SW620 cells. No substantial difference was observed in their fatty acid composition (Fig. 1). Hence, TG constitute the major lipid class that displays changes in FA composition in the SW620 cells when compared to the SW480 cells.

To understand the molecular mechanisms regulating these changes in the lipidomic profiles, we performed expression analyses (Fig. 2) and also used a publicly accessible gene expression profile. Figure 3 was derived from our previously published review article (Munir *et al.*, 2019) and displays overview of the major cancer-associated lipid metabolism pathways. The fold-changes in the expression levels of various genes/enzymes are indicated with a colored box on the left-side of the respective gene symbol. For color codes see the color key

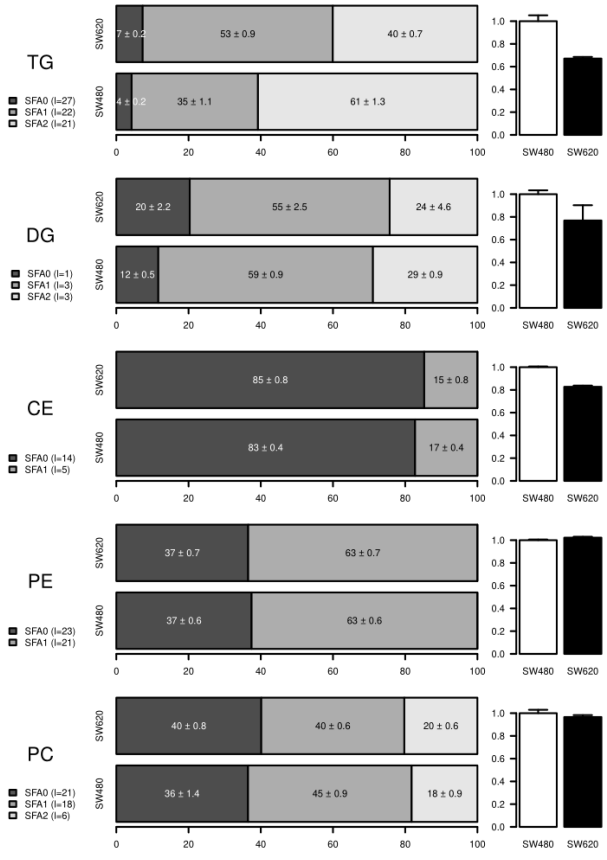

Figure 1. Fatty acid composition and saturation indices of major lipid classes.
The figure is structured in five rows and three columns. Rows show data for the major lipid classes: triglycerides (TG), diglycerides (DG), cholesterol esters (CE), Phosphatidylethanolamines (PE) and phosphatidylcholines (PC). The column on the left displays lipid class ID and a legend indicating the number of lipid-subspecies within each lipid class containing different numbers of saturated fatty acids (0, 1 or ≥2SFAs). Center column shows the relative amount (in percent of summed ion intensity) of lipid subspecies calculated in reference to the total amount of lipids within both SW cell lines. Numeric values for mean and standard deviation, calculated over 6 replicate samples per cell line, are given within the bars. The column on the right displays the saturation indices of the respective lipid classes normalized to SW480.

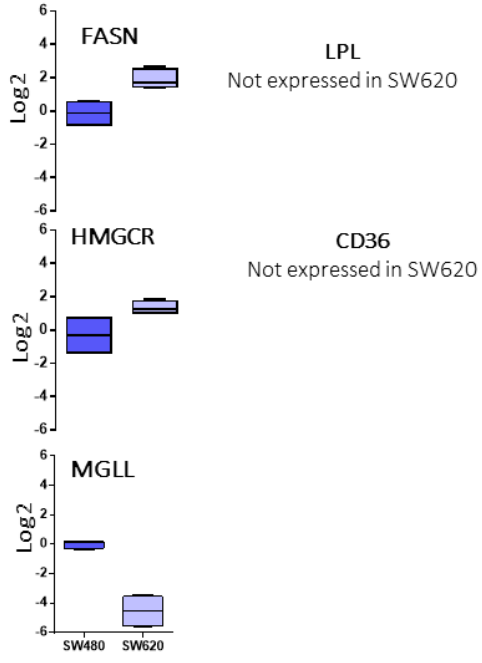

Figure 2. Expression of selected genes from de novo lipid synthesis or lipid uptake/degradation pathways in the SW480 and SW620 cell lines.
Box plots showing log2 transformed and median normalized values of FASN, HMGCR and MGLL. LPL and CD36 expressions were not detected. The levels of the different transcripts were measured in 3 to 6 samples by qPCR. The results show the distribution of corresponding transcripts relative to GAPDH, with the box indicating the 25th–75th percentiles, with the median indicated. The whiskers show the range.

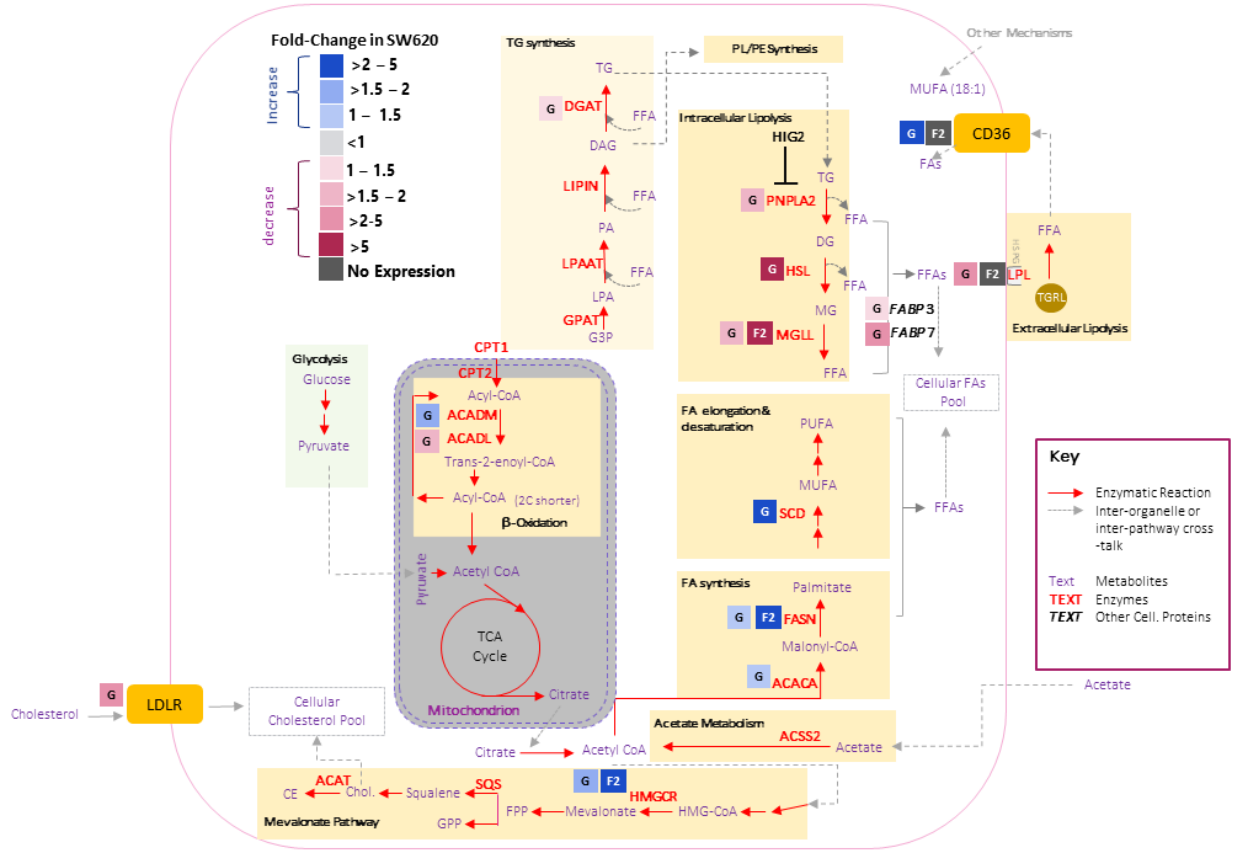

Figure 3. Fold-changes in expression levels of major lipid metabolism gene pathways.
Major lipid metabolism pathways are shown as boxes. The fold-changes in the expression levels of various genes/enzymes in the SW620 cells compared with the SW480 cells are indicated with a colored box on the *left-side* of the respective gene symbol. For color codes see color key at the *top-left* corner. The expression data for these analyses were extracted from the NCBI GEO database, accession number GSE2509. For some markers, gene expression analysis was performed (Fig. 2). The symbols within fold-change boxes represent the data source (G, GEO database; F2, Fig. 2).

at the top-left corner of Fig. 3. As discussed above, the difference in the FA composition of TG was the most significant difference between lipidomic profiles of the SW480 and SW620 cells, with SW620 cells displaying a significantly lower TG saturation-index. A recent study has shown that gene silencing of diglyceride acyltransferases (DGATs), enzymes that catalyze formation of TG from DGs and Acyl CoA, induces an increase in the TG saturation-index (Ackerman *et al.*, 2018). Hence, increased expression of DGAT might induce decreased SI in TG. Our analyses revealed that expression of DGAT was slightly decreased (1–1.5 Fold) in the SW620 cells (Fig. 3, TG Synthesis). Hence, DGAT expression might not be responsible for the changes in the TG saturation-index of the SW620 cells.

Next, we looked at other lipid metabolism pathways that have been implicated in regulation of the lipid saturation-indices. Highly active *de novo* FA synthesis induces increased SFAs or MUFAs levels in cancer cells (Rysman *et al.*, 2010). Expression of FA synthesis genes is up-regulated in the SW620 cells, hence this pathway may not be contributing to the decreased SI in these cells (Fig. 3, FA Synthesis).

Major genes of intracellular lipolytic pathway, including PNPLA2, HSL and MGLL, are all down regulated in the SW620 cells (Fig. 3, Intracellular Lipolysis). This may explain the dramatic increase in total triglyceride (TG) levels in the SW620 cells. However, specific decrease in ≥2 SFA containing TG could not be explained by this mechanism.

Expression of ACADM and ACADL, enzymes that catalyze the first step of FA oxidation in mitochondria, is differentially regulated in the SW620 cells. The expression of ACADM was up regulated, while the expression of ACADL was down-regulated in SW620, in comparison to the SW480 cells (Fig. 3, FA Oxidation). This observation is of special interest in this context, because ACADL is known to mediate unsaturated FA oxidation, whereas ACDM prefers saturated FAs as substrates. Hence, it is possible that in the SW620 cells there is an increased oxidation of SFAs, while decreased oxidation of unsaturated FAs. This may cause selective depletion of SFAs in the stored lipids and induce decreased SI of TG and CE. Recent studies have shown that disruptions in lipid metabolism or nutrient/oxygen supply also drastically affects the FA-composition of TG in cancer cells, while the FA-composition of other lipid classes is not significantly affected (Ackerman *et al.*, 2018; Lisec *et al.*, 2019). Hence, FA-composition of TG is most markedly affected by the changes in cancer stage, tumor microenvironment and de novo FA synthesis.

Conflict of interest

The authors declare no potential conflicts of interest.

REFERENCES

Ackerman D, Tumanov S, Qiu B, Michalopoulou E, Spata M, Azzam A, Xie H, Simon MC, Kamphorst JJ (2018) Triglycerides promote lipid homeostasis during hypoxic stress by balancing fatty acid saturation. *Cell Reports* **24**: 2596–2605. e2595

Fhaner CJ, Liu S, Ji H, Simpson RJ, Reid GE (2012) Comprehensive lipidome profiling of isogenic primary and metastatic colon adenocarcinoma cell lines. *Anal Chem* **84**: 8917–8926. https://doi.org/10.1021/ac302154g

Hewitt RE, McMarlin A, Kleiner D, Wersto R, Martin P, Tsokos M, Stamp GW, Stetler-Stevenson WG (2000) Validation of a model of colon cancer progression. *J Pathol* **192**: 446–454. https://doi.org/10.1002/1096-9896(2000)9999:9999<::Aid-path775>3.0.Co;2-k

Leibovitz A, Stinson JC, McCombs WB, 3rd, McCoy CE, Mazur KC, Mabry ND (1976) Classification of human colorectal adenocarcinoma cell lines. *Cancer Res* **36**: 4562–4569. PMID: 1000501

Lisec J, Jaeger C, Rashid R, Munir R, Zaidi N (2019) Cancer cell lipid class homeostasis is altered under nutrient-deprivation but stable under hypoxia. *BMC Cancer* **19**: 501. https://doi.org/10.1186/s12885-019-5733-y

Munir R, Lisec J, Swinnen JV, Zaidi N (2019) Lipid metabolism in cancer cells under metabolic stress. *Brit J Cancer* **120**: 1090-1098. https://doi.org/10.1038/s41416-019-0451-4

Pakiet A, Kobiela J, Stepnowski P, Sledzinski T, Mika A (2019) Changes in lipids composition and metabolism in colorectal cancer: a review. *Lipids Health Dis* **18**: 29. https://doi.org/10.1186/s12944-019-0977-8

Rysman E, Brusselmans K, Scheys K, Timmermans L, Derua R, Munck S, Van Veldhoven PP, Waltregny D, Daniëls VW, Machiels J, Vanderhoydonc F, Smans K, Waelkens E, Verhoeven G, Swinnen JV (2010) *De novo* lipogenesis protects cancer cells from free radicals and chemotherapeutics by promoting membrane lipid saturation. *Cancer Res* **70**: 8117–8126. https://doi.org/10.1158/0008-5472.CAN-09-3871

Schønberg SA, Lundemo AG, Fladvad T, Holmgren K, Bremseth H, Nilsen A, Gederaas O, Tvedt KE, Egeberg KW, Krokan HE (2006) Closely related colon cancer cell lines display different sensitivity to polyunsaturated fatty acids, accumulate different lipid classes and downregulate sterol regulatory element-binding protein 1. *FEBS J* **273**: 2749–2765. https://doi.org/10.1111/j.1742-4658.2006.05292.x

Tirinato L, Liberale C, Di Franco S, Candeloro P, Benfante A, La Rocca R, Potze L, Marotta R, Ruffilli R, Rajamanickam VP, Malerba M, De Angelis F, Falqui A, Carbone E, Todaro M, Medema JP, Stassi G, Di Fabrizio E (2015) Lipid droplets: a new player in colorectal cancer stem cells unveiled by spectroscopic imaging. *Stem Cells (Dayton, Ohio)* **33**: 35–44. https://doi.org/10.1002/stem.1837